SUPPLEMENTARY INFORMATION

Suppressed charge recombination via defect engineering of confined semiconducting quantum dots for photoelectrocatalysis

Ce Hu[1,3,#], Daojian Ye[1,2,#], Jie Ren[1,2,#], Congcong Wu[1,2], Chenya Zhao[1,2], Weiyang Xu[1,2], Hang Zhou[1,2], Ting Yu[1,2], Xingfang Luo[1,2,*] and Cailei Yuan[1,2,*]

[1]Jiangxi Key Laboratory of Nanomaterials and Sensors, Jiangxi Normal University, 99 Ziyang Avenue, Nanchang 330022, Jiangxi, China.

[2]School of Physics, Communication and Electronics, Jiangxi Normal University, 99 Ziyang Avenue, Nanchang 330022, Jiangxi, China.

[3]Analytical & Testing Center, Jiangxi Normal University, 99 Ziyang Avenue, Nanchang 330022, Jiangxi, China.

*Corresponding author. E-mail: xfluo@jxnu.edu.cn, clyuan@jxnu.edu.cn

[#]C.H., D.Y. and J.R. contributed equally to this work.

Keywords: Defect engineering; suppressed charge recombination; semiconducting QDs; photoelectrocatalytic oxygen evolution.

Experimental section

Catalyst preparation.

The defect-engineered semiconducting CuSe quantum confined catalysts were prepared via pulsed laser deposition (PLD) technique onto glassy carbon electrodes. PLD is a general method to prepare high quality ultrathin nanofilms by using pulsed laser ablation of target under ultrahigh vacuum conditions. Initially, the vacuum chamber was evacuated to 2.0×10^{-8} Torr. The removal of air (oxygen) to produce an ultrahigh vacuum growth condition is important for introducing abundant selenium vacancies by protecting CuSe quantum dots (QDs) from oxidation or degradation. Then, a KrF (248 nm) excimer laser with a laser energy of 300 mJ and a pulse frequency of 5 Hz was conducted. During the pulsed laser ablation, the target was rotated slowly and the physically combined carbon target (high purity of 99.99%) and CuSe target (high purity of 99.99%) were scanned alternately. As a result, the defect-engineered CuSe QDs were formed in amorphous carbon matrix at the substrate temperature of 400℃. The substrate temperature is critical to crystallization kinetics. The CuSe QDs with different size are prepared at different substrate temperatures. As shown in Figure S6, with decreasing substrate temperature, the CuSe QDs size is gradually decreased. For catalysis, the high specific surface area is favourable. Since the CuSe QDs prepared at 400℃ have the smallest grain size while maintaining high crystalline quality as evaluated by characterizations, then 400℃ was chosen as the optimal substrate temperature. Note that as the substrate temperature decreased further from 400℃, the crystalline quality deteriorated. After PLD deposition, the CuSe quantum confined catalysts were naturally cooled down to room temperature under the base pressure. The CuSe QDs size can be tailored by adjusting the precursors ratio of CuSe to carbon. And for photoelectrochemical characterizations,

the thickness of PLD-prepared defect-engineered CuSe quantum confined catalysts is about 10 nm. In addition, the pristine CuSe quantum confined catalysts were obtained by healing the selenium vacancies in the defect-engineered CuSe QDs through rapid thermal annealing (400℃ for 120 s) in selenium atmosphere.

Sample characterizations.

Transmission electron microscopy (TEM) images were recorded with JEM-2010 microscope (JEOL Ltd.). And TEM electron diffraction pattern was simulated by JEMS software. X-ray diffraction pattern was recorded using a X'Pert3 powder X-ray diffractometer with Cu Kα radiation. UV-vis absorption spectrum in the region of 200-800 nm was recorded on a Shimadzu UV-2550 spectrophotometer. X-ray photoelectron spectroscopy spectra were performed on a Kratos Axis Ultra DLD spectrometer with Al Kα radiation. And the binding energies were calibrated by referencing C 1s of 284.8 eV. Electron paramagnetic resonance spectra at X-band (9.85 GHz) were obtained using a Magnettech A300 EPR spectrometer. Room-temperature PL and Raman spectra were acquired using a HORIBA Scientific LabRAM HR Evolution system under 514 nm laser excitation. Electrical transport characteristics were performed on a physical property measurement system (Quantum Design EVERCOOLII, Inc.) with a combination of SourceMeter (Keithley Model 2636B) and Nanovoltmeter (Keithley Model 2182A).

Photoelectrocatalysis characterizations.

Photoelectrocatalysis characterizations were performed using a three-electrode system with CH Instrument electrochemical analyzer (model CHI760E). CuSe quantum confined nanocomposites on glassy carbon substrates were acted as the working electrodes. Glassy carbon needle and saturated Hg/HgO were respectively acted as counter electrode and reference electrode. All potentials were converted to potentials

versus reversible hydrogen electrode (RHE) reference scale (Figure S7). The impedance spectra were measured in the range of 0.1-10^5 Hz with a perturbation voltage of 5 mV. A 1000 W high pressure Xenon light source was used to simulate the solar illumination and to give an irradiance of about 15 mW·cm^{-2} at the surface of the working electrode. The irradiance measurement was conducted by using a FZ-A illuminance meter of Beijing Normal University Optoelectronic Instrument Factory. All photoelectrochemical characterizations were performed in 1 M KOH aqueous solution without the addition of sacrificial agent at room temperature.

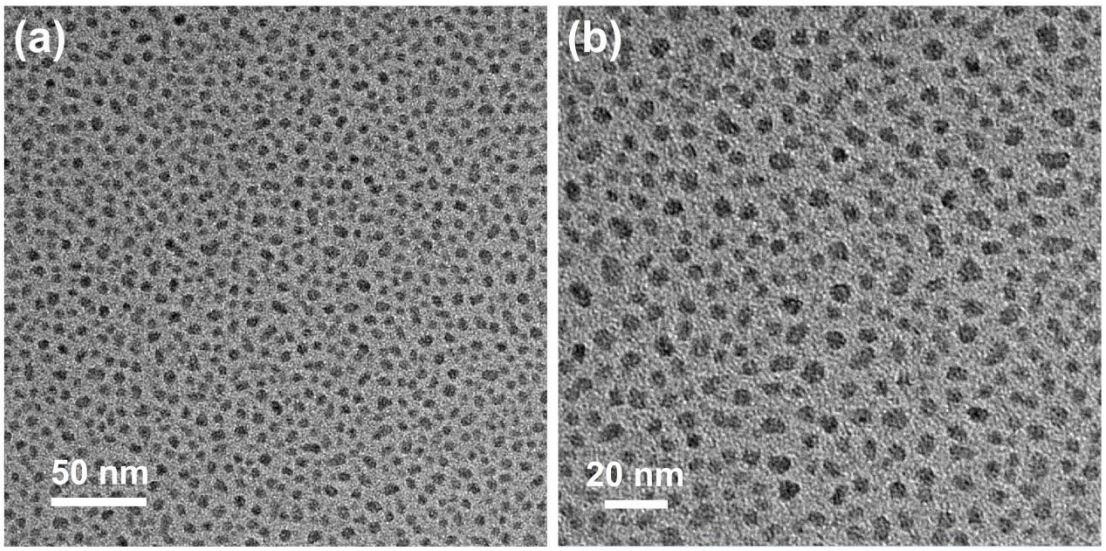

Supplementary Fig. 1. Low-resolution TEM (LRTEM) images of defect-engineered CuSe QDs.

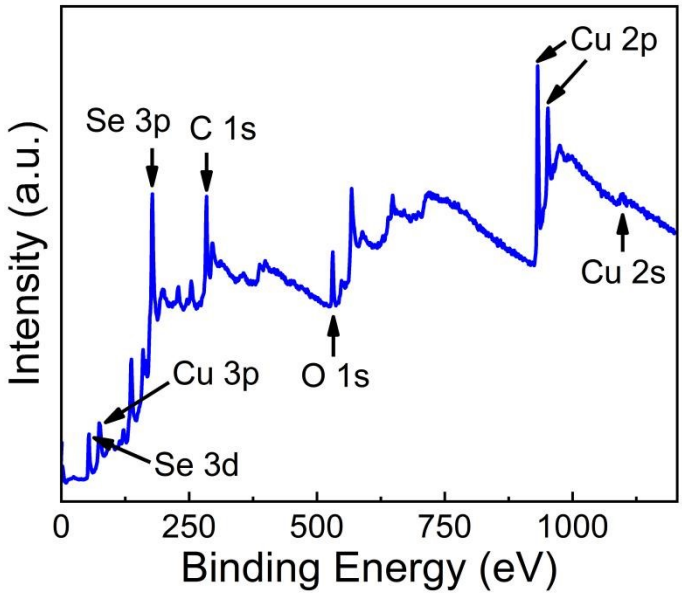

Supplementary Fig. 2. Overall X-ray photoelectron spectroscopy spectrum of defect-engineered CuSe QDs.

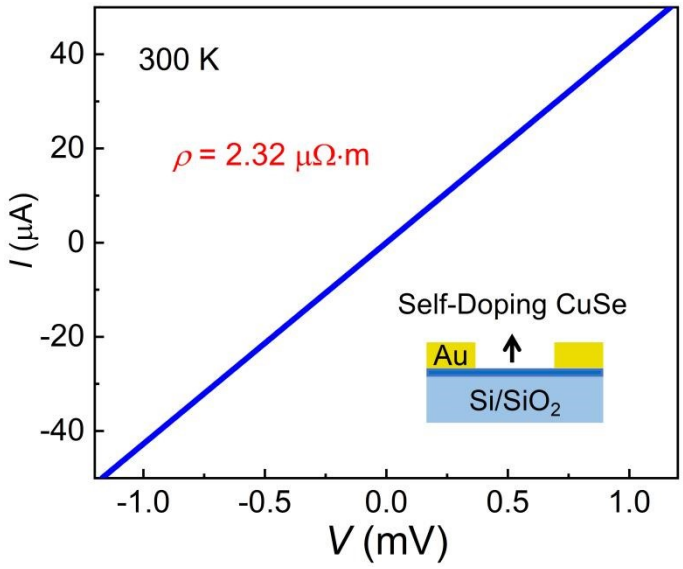

Supplementary Fig. 3. Current-voltage curve at room temperature. Inset shows the schematic diagram of the device for electrical transport measurements.

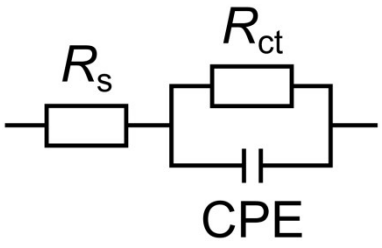

Supplementary Fig. 4. The equivalent circuit to fit the electrochemical impedance spectroscopy of oxygen evolution reaction process. Interpretation of EIS measurements is usually done by correlation between impedance data and equivalent circuits, which represent the physical processes occurring in the system. Randles equivalent circuits are widely used in many electrochemical systems. In view of the non-ideal characteristics of capacitor, a constant phase element (CPE) is introduced into the equivalent circuit to improve the measurement accuracy of capacitance and resistance.

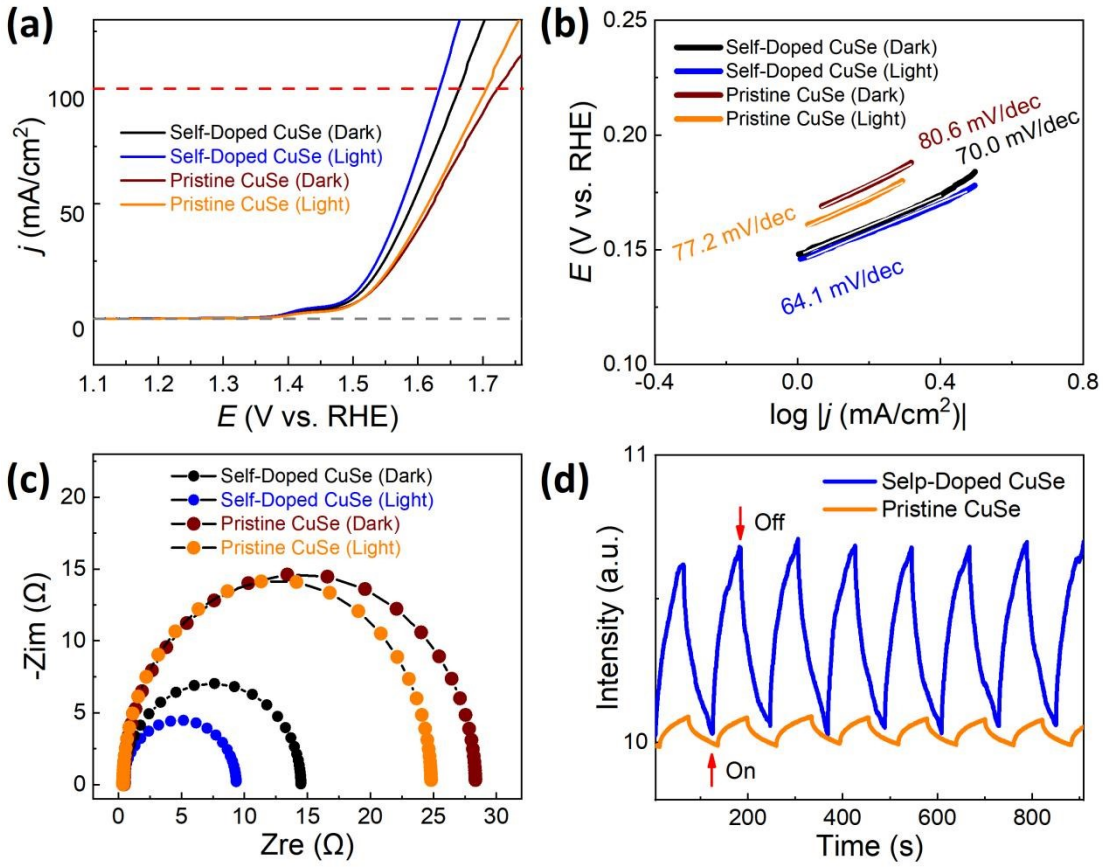

Supplementary Fig. 5. (a) LSV curves, (b) corresponding Tafel plots, and (c) Nyquist plots of pristine and self-doped CuSe QDs with and without solar illumination. (d) Time-resolved photo-response to the periodic solar illumination of pristine and self-doped CuSe QDs.

The comparison of photoelectrocatalytic OER activity was made for the self-doped CuSe QDs with the pristine CuSe QDs.

OER performance comparison without solar illumination.

As shown in **Figure S5a**, the OER property of self-doped CuSe QDs without solar illumination (276 mV at 10 mA/cm^2) is obviously better than that of pristine CuSe QDs (297 mV at 10 mA/cm^2). This is because the self-doped CuSe QDs possess high-density catalytic active sites as the consequence of abundant non-saturated bonds associated with Se vacancies. And the corresponding Tafel slope (**Figure S5b**) of self-doped CuSe QDs (70 mV·dec^{-1}) is lower than that of pristine CuSe QDs (80.6 mV·dec^{-1}), indicating the faster OER kinetics of self-doped CuSe QDs due to the

increase of valence band maximum (VBM) since the valence band structure near the Fermi level is crucial to the OER kinetics.[1] With the presence of abundant Se vacancies in CuSe semiconducting QDs, VBM value increases from 1.76 to 2.01 eV (Figure 2b in the main text shows the valence band characterizations) as the consequence of n-type self-doping. The abundant Se vacancies, acting as electron donors, will lead to the Fermi level shifts toward the conductive band minimum, and the electrical conductivity is thus increased correspondingly which is favourable to OER kinetics. Accordingly, it can be seen from **Figure S5c** that self-doped CuSe QDs have smaller charge transfer resistance (R_{ct}), which means higher electron and mass transfer efficiency.

OER photoelectrocatalytic activity comparison with solar illumination.

Under the stimulation of solar illumination, the improvement of OER electrocatalytic performance for pristine CuSe QDs is obviously smaller than that of self-doped CuSe QDs (**Figure S5a** and **S5b**), which is due to the high photogenerated charge carriers recombination rate of pristine CuSe QDs. Moreover, **Figure S5d** shows the time-resolved photo-response to the periodic solar illumination. Compared with the distinct light-operated switching behavior of self-doped CuSe QDs, the switching behavior of pristine CuSe QDs is mediocre, demonstrating that the Se vacancies is crucial for the photo-enhanced electrocatalytic behaviour. The suppression of photogenerated charge recombination by the trapping states associated with Se vacancies resulted in the high photoelectrochemical efficiency of self-doped CuSe QDs, which is conductive to photoelectrocatalytic activity.

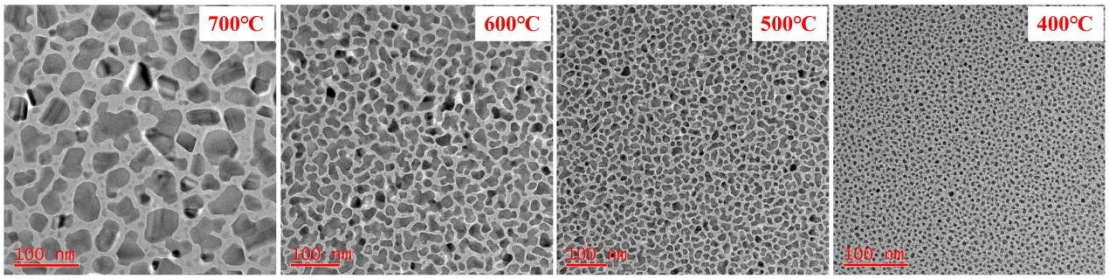

Supplementary Fig. 6. LRTEM images of CuSe QDs prepared at different substrate temperatures.

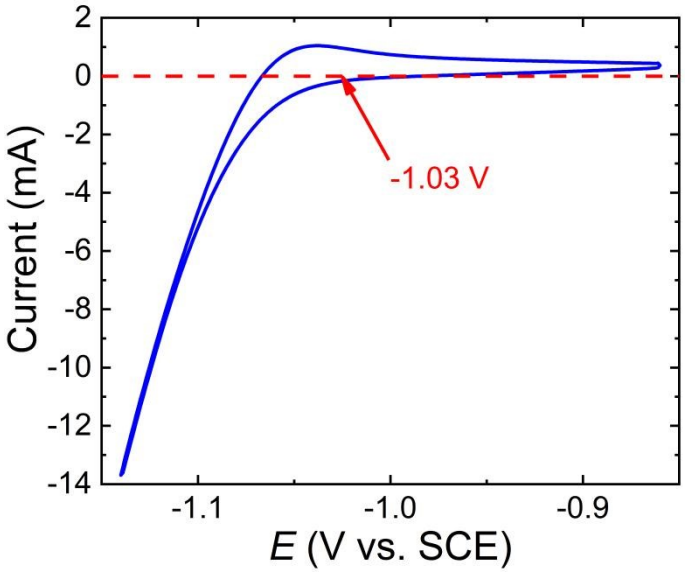

Supplementary Fig. 7. Calibration of reference electrode.

Table S1. Comparison of OER activities for the defect-engineered CuSe QDs catalyst with other CuSe-based OER electrocatalysts.

Electrocatalyst	**Electrolyte**	**Overpotential (mV) at 10mA/cm^2**	**Tafel slope (mV/dec)**	**Reference**
CuSe QDs under illumination	**1.0 M KOH**	**268.0**	**64.1**	**This work**
$(Co_{0.21}Ni_{0.25}Cu_{0.54})_3Se_2$	1.0 M KOH	272.0	53.3	[1]
Cu_2Se (Hydrothermal method)	1.0 M KOH	290.0	136.7	[2]
CuSe	1.0 M KOH	297.0	89.0	[3]
CuCoSe@NC	1.0 M KOH	300.0	80	[4]
Cu_2Se (CVD)	1.0 M KOH	300.0	90.9	[2]
Cu_3Se_2	1.0 M KOH	326	82.9	[1]
Cu_2Se-Cu_2O	0.2 M carbonate buffer	465	140	[5]

References:

[1] Cao, X. et al. Identifying hgigh-efficiency oxygen evolution electrocatalysts from Co-Ni-Cu based selenides through combinatorial electrodeposition. *J. Mater. Chem. A* **7**, 9877-9889 (2019).

[2] Masud, J. et al. Copper selenides as high-efficiency electrocatalysts for oxygen evolution reaction. *ACS Appl. Energy Mater.* **1**, 4075-4083 (2018).

[3] Chakraborty, B. et al. Crystalline copper selenide as a reliable non-noble electro(pre)catalyst for overall water splitting. *ChemSusChem* **13**, 3222-3229 (2020).

[4] Zhang, H. et al. In situ encapsulation engineering boosts the electrochemical performance of highly graphitized N-doped porous carbon-based copper–cobalt selenides for bifunctional oxygen electrocatalysis. *Nanoscale* **13**, 17663-17674 (2021).

[5] Chen, H. et al. A Cu_2Se-Cu_2O film electrodeposited on titanium foil as a highly active and stable electrocatalyst for the oxygen evolution reaction. *Chem. Commun.* **54**, 4979-4982 (2018).